Excluding Ionospherically Unsafe Satellite Geometries in GBAS CAT-I

Oscar Bria, Javier Giacomantone, and Luciano Lorenti

Research Institute in Computer Science (III-LIDI) - School of Computer Science
National University of La Plata - Argentina
onb@info.unlp.edu.ar

Abstract. We show the results of the implementation of a preliminary algorithm for excluding ionospherically unsafe satellite geometries in Ground-Based Augmentation Systems Category I. Minimum knowledge of the ionospheric treat model is assumed and the assistance of the code-carrier divergence monitor is not considered. All the satellites in view above 5° in elevation are included in the computations. The inflation of the standard deviation of the vertical ionospheric gradient implements the exclusion. Full availability remains for a typical day in the site of La Plata Airport.

Keywords: GBAS Category I, Ionospheric Threat, Parameter Inflation.

1 Introduction to GBAS

Ground-Based Augmentation System (GBAS) is a system that provides differential corrections and integrity monitoring of Global Navigation Satellite Systems (GNSS) signals for navigation and precision approach service in the vicinity of the host airport. GBAS yields the accuracy, integrity, continuity and availability necessary for Category I, and eventually Category II, and III precision approach operations [1, 2].

The system consists of three parts: 1) the satellite signal in space (SIS) coming from one or several GNSS constellations; 2) the local Ground Facility (GGF) equipped normally with four satellite receivers, processing equipment and a VHF data broadcast (VDB) transmitter; and 3) the aircraft devices related to the multi-mode receiver (MMR).

The GGF provides the aircraft with approach path data and, for each satellite in view, geo-referenced range corrections and integrity information. The corrections enable the aircraft to determine its position relative to the approach path more accurately. Under nominal conditions these corrections are considered practically the same for the ground station and for the aircraft. That is, the basic assumption of GBAS is that errors have a high local correlation.

Integrity is the function of a system that warns users in a timely manner when the system or some part of it should not be used. The integrity function prevents severe risks, eventually affecting system continuity and availability [3]. In GBAS Category I (CAT-I) the responsibility for integrity resides exclusively

in the GGF. Verification and certification of GBAS integrity is based on the analysis of extremely rare events which can lead to large positioning errors. These events are generally only dealt theoretically or by simulation [4, 5]. The most important of these rare effects are strong ionospheric gradients, which are not directly recognized by the GGF by any intended means. Hence the importance of being able to foresee and mitigate the effects of this anomalies in some way [6]. Excluding unsafe geometries is one of such ways; ionospheric field monitor is other alternative [7].

2 Protection Levels, Alert Limits and Position Errors

As mentioned, for GBAS CAT-I the GGF is designed to guarantee the integrity of each broadcasted correction by monitoring, in diverse ways, each related satellite measure to ensure that the correction error is bounded. If that is not the case the satellite is declared unsafe. The nominal correction error standard deviation for each satellite $\sigma_{\mathrm{pr}_{\mathrm{gnd}},i}$ $[m]$ as seen from ground, and the nominal standard deviation of the vertical ionospheric gradient σ_{vig} $[m/m]$ coming from site studies, are also broadcasted.

Based on the information received from the GGF and also based in own data, the aircraft computes horizontal and vertical protection levels (HPL and VPL) for the measurements for each epoch (every 0.5 second). Particularly VPL are safe if they are bellow the vertical alert limit (VAL). For GBAS CAT-I precision approach operations VAL = 10 m at the minimum decision height of 200 ft that occurs at 6 km from the runway during landing.

If VPL is larger than VAL an integrity alert is generated. VPL is supposed to exceed the real unknown vertical position error (VPE). If VPE is larger than VPL but smaller than VAL the information is misleading. If VPE is larger than VPL and also larger than VAL the information is hazardously misleading.

The aircraft computes VPL as follow (see [8] for details):

$$\mathrm{VPL} = K_{\mathrm{ffmd}} \sqrt{\sum_{i}^{N} S_{\mathrm{vert},i}^2 \sigma_i^2} \ . \tag{1}$$

$$\sigma_i^2 = \sigma_{\mathrm{pr}_{\mathrm{gnd}},i}^2 + \sigma_{\mathrm{iono},i}^2 + \sigma_{\mathrm{air},i}^2 + \sigma_{\mathrm{tropo},i}^2 \ , \tag{2}$$

$$\sigma_{\mathrm{iono},i} = F_i \sigma_{\mathrm{vig}} (x_{\mathrm{aircraft}} + 2\tau v_{\mathrm{aircraft}}) \ , \tag{3}$$

$$\sigma_{\mathrm{air},i}^2 = \sigma_{\mathrm{multipath},i}^2 + \sigma_{\mathrm{noise},i}^2 \ . \tag{4}$$

$S_{\mathrm{vert},i}$ is the vertical position component of the weighted-least-squares projections matrix for satellite i (see equation (8)). N is the number of satellite in-view for the present epoch.
K_{ffmd} is the multiplier that determines the required probability of fault-free missed detection.

σ_i^2 is the variance of a normal distribution overbounding the range domain error distribution for satellite i for the fault-free hypothesis H_0 (see [9]).
$\sigma^2_{\mathrm{pr}_{\mathrm{gnd}},i}$ is the fault-free variance of the ground error term associated with the correction for satellite i.
$\sigma_{\mathrm{iono},i}$ is the ground residual ionospheric uncertainty for satellite i. F_i is the vertical-to-slam obliquity factor for satellite i. σ_{vig} is the standard deviation of a normal distribution of the residual ionospheric uncertainty due to nominal spatial decorrelation (a typical value is 4 mm/km). The following factor has two components, the horizontal distance from GGF to aircraft (x_{aircraft}), and a synthetic distance produced by a smoothing filter used to mitigate multipath and noise with a time constant τ of 100 s. v_{aircraft} is the velocity of the aircraft in the direction of the airport.
For details on $\sigma^2_{\mathrm{air},i}$ and $\sigma^2_{\mathrm{tropo},i}$ see the above last references.
In the above set of equations is not included the vertical protection level under a single-satellite (satellite i) ephemeris fault, however it is considered in the computations. Failures of the hypothesis H_1 [10] are not relevant to excluding geometries [11].

3 Ionospheric Threat and Tolerable Error Limit

GPS satellites fly in medium Earth orbits (MEO) at an altitude of approximately 20200 km. The ionosphere is a region of the atmosphere located about 50 – 1000 km above the Earth's surface. In this region, solar radiation produces free electrons and ions that cause phase advances and group delays to GPS radio waves.

Ionospheric fronts (also called ionospheric storms) pose a significant threat to single frequency ground based augmentation systems (GBAS) for airplane precision approach because they can produce differential delays between the aircrafts and the GGF that are not detected in time to generate an integrity alert [12]. That is, uncorrelated delays could produce misleading and hazardously misleading situations. Ionospheric fronts are recommended [13] to be modeled by a moving wedge form with four parameters [1], including the maximum ionospheric spatial gradient for a particular region [14].

The first wedge model has been parameterized for the conterminous U.S. (CONUS) where ionspheric delay gradients as large as 435 mm/km have been observed [15]. In the Brazil ionosphere the largest gradient of about 850 mm/km has been registered [16]. There are not known developments of ionospheric threat wedge model for Argentina.

The development and utilization of the ionospheric threat model occurs in two stages [17]. The first stage is observation, in which data accumulated over a lengthy period (usually including the greatest activity of a solar cycle) is collected to describe and cover the features of ionosphere impact on GBAS [18]. The

[1] The four paramenters are: spatial gradient, front moving speed, width and maximum delay [11].

results of observation are used to estimate the bounding parameters of the threat model. The second stage is simulation, in which the completed threat model is used in a simulation including the GGF and user operation. The simulations provide estimations of the integrity risk (particularly the hazardously misleading information (HMI) analyses [19]), the availability, and the impact to the ground and airborne monitors.

Equation (3) gives the magnitude of ionospheric range error in slant direction under steady-state conditions. The distance for decision hight (DH) for CAT-I is 6 km away from the GGF. For a nominal σ_{vig} of 4 mm/km the error is bounded by 0.24 m, in about 99.8 % of the cases. Meanwhile an anomalous large ionospheric delay gradient of 425 mm/km could produce certainly a range error as large as 8.5 m.

The maximum vertical position error due to the worst-case user error induced by an ionosphere anomaly (as estimated by the ground subsystem) need only be bounded by a tolerable error limit (TEL) that luckily is greater than VAL [11, 15, 20, 21].

Several criteria have been proposed to establish a value for TEL. In [21] the obstacle clearance surface (OCS) concept is used to assess the safety of a CAT-I approach if an ionospheric anomaly produces vertical navigation errors. A maximum vertical error of about 29 m would be allowable at the nominal DH of 200 ft.

4 Algorithm Description

We followed [11, 15, 22, 23] as references for the algorithm implementation. The algorithm produces an inflation factor that depends of current satellite geometry. Inflation factors larger than 1 are applied to σ_{vig} when it nominal value do not produce a VPL that exceeds VAL when the possible error is not bounded by TEL. This mechanism excludes unsafe geometries for been considered by the aircraft.

The algorithm has four principal computational steps: 1. *GGF and Subset Geometries*, 2. *Ionosphere-Induced Range Error*, 3. *Ionosphere-Induced Vertical Error* and 4. *Parameter Inflation*.

4.1 GGF and Subset Geometries

Satellites that are visible to the GGF may not be included in the positioning solution of an approaching airplane. It is assumed that up to two satellites from the all-in-view satellite at the ground facility are not used by the airborne [2]. If there are N satellites visible to the GBAS ground facility, there are

$$\sum_{k=N-2}^{N} \binom{N}{k} \tag{5}$$

[2] The minimum number of satellites to be used by the airborne is four.

subset satellite geometries from the set of N satellites visible to the GGF. Figure 1 shows the evolution fo the number od satellites in view. Figure 2 shows an example with nine satellites in view at a given epoch, the total number of subset geometries to consider in this case is, $\sum_{k=7}^{9} \binom{9}{k} = 46$.

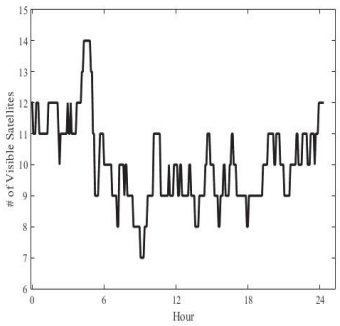

Fig. 1. Evolution of the number of visible satellites above 5° during a 24 hours typical period for a GBAS Ground Facility as if it was located at La Plata Airport (34.9655° S, 57.8954° W).

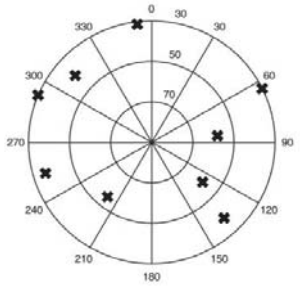

Fig. 2. Diagram of satellite positions over the sky above 5° (actually above 30° in this case) from the GBAS Ground Facility point of view. Nine satellite are in view for the current epoch.

4.2 Ionosphere-Induced Range Error

The closed-form approximation of the ionosphere-induced differential range error is:

$$\varepsilon = g \times (x_{\text{aircraft}} + 2\tau v_{\text{aircraft}}) \ . \tag{6}$$

ε is the ionosphere-induced differential range error $[m]$.
g is the ionospheric gradient $[mm/km]$.
x_{aircraft} is the separation between the GGF and the approaching airplane $[km]$.
τ is the time constant of the carrier-smoother filter $[s]$.
v_{aircraft} is the velocity of the approaching airplane $[km/s]$.

Given an airplane at a certain distance and with certain velocity equation (6) represents the worse case for a given g. In the bibliography (e.g., [24]) considerations are taken about the relative velocity between the ionospheric front and the particular satellite, and the preventive action of the code-carrier divergence (CCD) monitor is considered [25]. Neither of those advantages are taken here to possible reduce the range error ε for every satellite for a particular geometry.

4.3 Ionosphere-Induced Vertical Error

Given airplane and ionosphere front movement geometries, a large ionospheric gradient may be unobservable to the GGF and meanwhile affecting the airplane

that is not conveniently prevented of the integrity risk. While an airplane is approaching a runway, an ionospheric front can impact the SIS of two satellites ($k1$ and $k2$) simultaneously. Hence the worst case ionospheric error in vertical (IEV) for any pair of satellite of a given geometry for a particular epoch can be expressed as follows [3],

$$\mathrm{IEV}_{k1,k2} = |S_{\mathrm{vert},k1}\varepsilon_{k1}| + |S_{\mathrm{vert},k2}\varepsilon_{k2}| \ . \tag{7}$$

$$S = (G^T W G)^{-1} G^T W \ . \tag{8}$$

$$G_i = [-\cos \mathrm{El}_i \cos \mathrm{Az}_i \ -\cos \mathrm{El}_i \sin \mathrm{Az}_i \ -\sin \mathrm{El}_i \ 1] \ . \tag{9}$$

$$W^{-1} = \begin{bmatrix} \sigma_1^2 & 0 & \dots & 0 \\ 0 & \sigma_2^2 & \dots & 0 \\ \vdots & \vdots & \ddots & \vdots \\ 0 & 0 & \dots & \sigma_N^2 \end{bmatrix} \ . \tag{10}$$

Where $S_{\mathrm{vert},ki}$ is the vertical position component of the weighted-least-squares projection matrix S for satellite ki (see [8]), this component is dependent of satellite geometry (number of satellite in view and their spatial distribution referred to the GBAS local ground station) at each epoch; G_i is the row of the observation matriz G for satellite i; Az_i and El_i are the azimuth and elevation of satellite i (see Figure 2); W^{-1} is the inverse of the least square weighting matrix; and σ_i is the variance of a normal distribution that overbounds the true VPE distribution for satellite i under the fault-free hypothesis.

The IEV for every pair of each subset geometry considered for the approaching airplane is calculated and compared to obtain the maximum IEV (MIEV) for each geometry in a particular epoch. The number of pairs to be compared for each subset geometry with k satellites is

$$\binom{k}{2} \ . \tag{11}$$

Figure 3 shows and example of MIEVs compared with TEL.

Figure 4 shows the nominal VPLs at the same epoch as Figure 3. The subset geometries with VPL exceeding VAL are not approved by the airplane and they can not cause integrity failures even though their MIEVs a greater than TEL.

4.4 Parameter Inflation

From Figures 3 and 4 can be observed that some geometries exceeding TEL does not exceed VAL. In those cases exist potentially hazardous geometries not excluded by the integrity mechanism supported by the VPL computated with the nominal σ_{vig} broadcasted (see equations (1) and (3)).

[3] A less constrained expression for IEV is presented in [22].

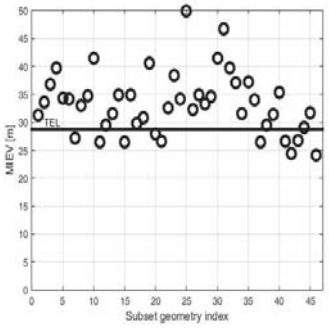

Fig. 3. MIEV for 29 subset geometries given 7 satellites in view. The 11 subset geometries exceeding TEL are potentially hazardous for this epoch.

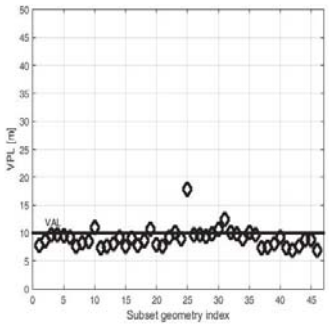

Fig. 4. Nominal VPL at the same epoch as Figure 3. The subset geometries with VPL exceeding VAL can not cause integrity failures.

If the GGF inflates the bradcasted parameters above their nominal values the airborne VPL increase as well. The most effective parameter to inflate is σ_{vig} which increase σ_i^2.

To obtain the minimum σ_{vig} needed for an epoch, VPLs are pre-computed by the GGF iteratively increasing a inflation factor I_{vig} until all hazardous geometries are properly removed. Some particular considerations have to be made to make the computation but exceed the limits of this explanation (see [22, 24]). The new inflated σ_{vig} is broadcasted to the airplane. As Figure 5 shows, all hazardous geometries exceeding TEL are excluded after inflation.

5 Algorithm Test

The algorithm implementation was tested for the location coordinates of La Plata Airport taken samples of recorded ephemeris every minute of a typical day. The assumed position of the aircraft is the decision point at 200 ft of elevation. An effective separation of 20 km results from the sum of the actual distance of 6 km between the reference station and the user, and the 14 km of synthetic separation generated by the memory of the code-carrier smoothing filter used to mitigate multipath error and code noise [8][4]. The nominal value of $\sigma_{\text{vig}} = 4.0 \;\; mm/km$. VAL $= 10$ m for approaching operations. The only parameter of the threat model to be considered is the maximum ionospheric gradient $g = 400 \;\; mm/km$.

Figure 6 shows the inflation factor I_{vig}. The inflated σ_{vig} can not exceed the maximum allowed broadcast value of 25.5 mm/km [26], meaning that in this case the maximum permitted value of $I_{\text{vig}} = 6.375$.

[4] A contant velocity of 0.07 km/s is assumed during the approach. The time constant of the carrier-smothing filter is $\tau = 100$ s.

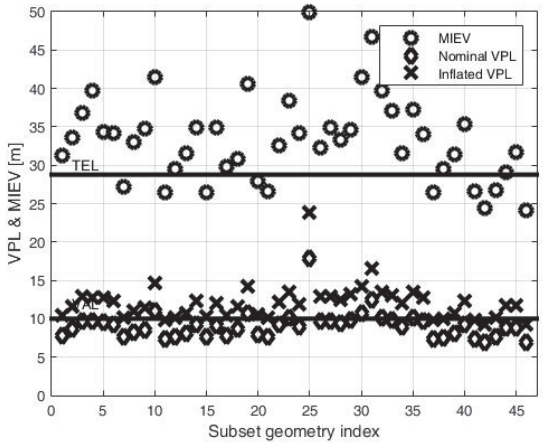

Fig. 5. Satellite geometry exclusion by σ_{vig} inflation. All hazardous geometries exceeding TEL are excluded after inflation.

By applying inflation factors to σ_{vig} all potentially hazardous geometries (and many more acceptable geometries) are eliminated from the approved set of geometries. Hence, system integrity is guaranteed by reducing system availability. Figure 7 shows the inflated VPL for the conditions of the test. The availability in this case remains 100 %.

6 Conclusions

It is difficult to improve integrity into existing systems while retaining sufficient availability to make the applications viable. As Pullen stated, these challenges are more than mathematical and require more than simply adding redundancy to mitigate the effects of individual failures [27].

Most of the anomalies affecting GBAS can be detected by the monitors founded in the CAT-I ground facility. Even moderate ionospheric anomalies are detected by the CCD and the clock acceleration monitors [12]. However, the worst-case ionospheric anomalies require additional mitigation techniques. The technique used here excludes possible hazardous geometries.

Equations (1) and (7) generate bounds too conservative to represent the wedge threat model and to accurately model the more realistic geometry and monitoring conditions found in practice. Nevertheless, the implementation shows that the availability is optimal for the site of La Plata Airport. This is due to the well suited geometry conditions, particularly the relatively large number of satellite always in view above 5° in elevation, as is observed in Figure 1.

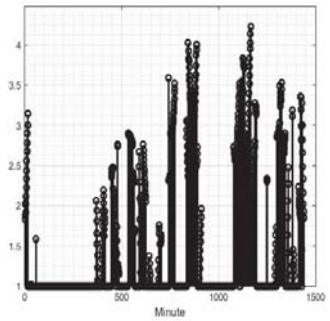

Fig. 6. Inflation factor I_{vig} for a 24 hours period. The broadcasted σ_{vig} is the inflation factor times the nominal $\sigma_{\text{vig}} = 4 \ \ mm/km$.

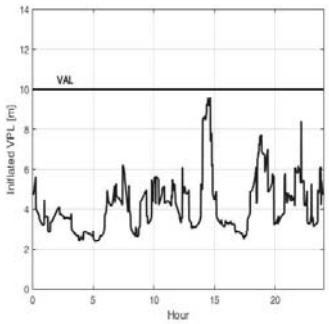

Fig. 7. Inflated VPL at La Plata airtport for a typical day. Availability is 100 % for a DH at 6 km using all the satellite in view.

References

1. International Civil Aviation Organization (ICAO): International Standards, Recommended Practices and Procedures for Air Navigation Services Annex 10 (1985)
2. U S Federal Aviation Administration (FAA): Specificaction Performance Type One Local Area Augmentation System Ground Facility. FAA-E-2937A (2002)
3. Rinnan, A., Gundersen, N., Sigmond, M., Nilsen, J.: Operational GNSS Integrity. In: Dynamic Positioning Conference (2011)
4. Dautermann, T., Sgammini, M., Pullen, S.: GBAS Ionospheric Threat Analysis using DLRs Hardware Signal Simulator. In...
5. SANJEEV Gunawardena, S., Zhu, Z., De Haag, M., Graas, F.: Remote-Controlled, Continuously Operating GPS Anomalous Event Monitor. In: Journal of the Institute of Navigation (2009)
6. Park, Y., Pullen, S., Enge P.: Enabling LAAS Airport Surface Movement: Mitigating the Anomalous Ionospheric Threat. In: IEEE/ION, Position, Location, And Navigation Symposium (2010)
7. Suzuki, S., Nozaki, Y., Ono, T., Yosihara, T., Saitoh, S., Sonosuke Fukushima, S.: CAT-I GBAS Availability Improvement through Ionosphere Field Monitor (IFM). In Proceedings of the 24th International Technical Meeting of The Satellite Division of the Institute of Navigation (2011)
8. Radio Technical Commission for Aeronautics (RTCA): Minimum Operational Performance Standards for GPS Local Area Augmentation Systm Airborne Equipment. Tecnical Report DO253C (2008)
9. Radio Technical Commission for Aeronautics (RTCA): Minimum Aviation System Performance for theLocal Area Augmentation Systm. Tecnical Report DO245A (2004)
10. Elias, P., Saotome, O.: System Architecture-based Design Methodology for Monitoring the Ground-based Augmentatiom System, Category I – Integrity Risk. In: J. Aerosp. Technol. Manag., São José dos Campos (2012)
11. Lee, J., Pullen, S., Park, Y., Enge P., Brenner, M.: Position-Domain Geometry Screening to Maximize LAAS Availability in the Presence of Ionosphere Anomalies.

In: Proceedings of the 19th International Technical Meeting of the Satellite Division of The Institute of Navigation ION GNSS (2006)
12. Luo, M., Pullen, S., Akos, D., Xie, G., Datta-Barua, S., Walter, T., Enge P.: Assessment of Ionospheric Impact on LAAS Using WAAS Supertruth Data. In: Proceedings of the ION 58 th Annual Meeting (2002)
13. International Civil Aviation Orgaanization South American Office (ICAO-SAM): Guide for Ground Based Augmentation System Implementation (2013)
14. Pullen, S. Park Y., Enge, P.: The IMpact and Mitigation of Ionspheric Anomalies on Ground-Based Augmentation of GNSS. In: Radio Science (2009)
15. Pullen, S., Enge, P.: An Overview of GBAS Integrity Monitoring with a Focus on Ionspheric Spatial Anomalies. In: Indian Journal of Radio & Space Physics (2007)
16. Lee, J., Yoon, M., Pullen, S., Gillespie J., Mather, N., Cole, R., Rodrigues de Souza, J., Doherty, P., Pradipta, R.: Preliminary Results from Ionospheric Threat Model Development to Support GBAS Operations in the Brazilian Region. In: Proceedings of the 28th International Technical Meeting of The Satellite Division of the Institute of Navigation (2015)
17. International Civil Aviation Orgaanization Asia and Pacific Office (ICAO-APAC): GBAS Safety Assesment Guidance Related to Anomalous Ionospheric Conditions (2016)
18. Kim, M, Lee, J. Pullen, S., Gillespie, J.: Data Quality Improvement and Applications of Long-Term Monitoring of Ionospheric Anomalies for GBAS. In: Proceedings of ION GNSS (2012)
19. U.S. Federal Aviation Administration (FAA): Ground Based Augmentation System Performance Analysis and Activities Report. First Quarter Report (2017)
20. Murphy, T., Harris, M., Park, Y., Pullen, S.: GBAS Differentially Corrected Positioning Service Ionospheric Anomaly Errors Evaluated in an Operational Context. In: Proceedings of the 2010 International Technical Meeting of The Institute of Navigation (2010)
21. Shively, C., Niles, R.: Safety Concepts for Mitigation of Ionospheric Anomaly Errors in GBAS. In: Proceedings of the 2008 International Technical Meeting of The Institute of Navigation (2008)
22. Lee, J., Seo, J., Park, Y., Pullen, S., Enge, P.: Ionospheric Threat Mitigation by Geometry Screening in Ground-Based Augmentation Systems. In: Journal of Aircraft (2011)
23. Vemuri, S., Sarma,. A., Redd, A., Reddy D.: Investigation of the Effect of Ionospheric Gradient on GPS Signals in the context of LAAS. In: Progress in Electromagnetics Research B (2014)
24. Seo,. J., Lee, J., Pullen, S., Enge, P., Close, S.: Trageted Parameter Inflation Within Ground-Based Augmentation Systems to Minimizw Anomalous Ionospheric Impact. In Journal of Aircraft (2012)
25. Simili, D., Pervan, B.: Code-Carrier Divergence Monitor for the GPS Local Area Augmentation System. In: IEEE/ION, Position, Location, And Navigation Symposium (2006)
26. Radio Technical Commission for Aeronautics (RTCA): Minimum Operational Performance Standards for GPS Local Area Augmentation Systm Airborne Equipment. Tecnical Report DO246D (2008)
27. Pullen, S.: Lessons Learned from the Development of GNSS Integrity Augmentations. In: Coordinates, `http://mycoordinates.org` (2016)